J|A|C|S
ARTICLES
Published on Web 07/22/2006

Construction of Segregated Arrays of Multiple Donor and Acceptor Units Using a Dendritic Scaffold: Remarkable Dendrimer Effects on Photoinduced Charge Separation

Wei-Shi Li,*,† Kil Suk Kim,§ Dong-Lin Jiang,† Hiroyuki Tanaka,# Tomoji Kawai,# Jung Ho Kwon,§ Dongho Kim,*,§ and Takuzo Aida*,†,‡

Contribution from the ERATO-SORST Nanospace Project, Japan Science and Technology Agency (JST), National Museum of Emerging Science and Innovation, 2-41 Aomi, Koto-ku, Tokyo 135-0064, Japan, The Institute of Scientific and Industrial Research (ISIR), Osaka University, 8-1, Mihogaoka, Ibaragi, Osaka 567-0047, Japan, National Creative Research Initiatives, Center for Ultrafast Optical Characteristics Control and Department of Chemistry, Yonsei University, Seoul 120-749, Korea, and Department of Chemistry and Biotechnology, School of Engineering, and Center for NanoBio Integration, The University of Tokyo, 7-3-1 Hongo, Bunkyo-ku, Tokyo 113-8656, Japan

Received May 3, 2006; E-mail: li@nanospace.miraikan.jst.go.jp; dongho@yonsei.ac.kr; aida@macro.t.u-tokyo.ac.jp

Abstract: Dendritic molecules appended with multiple zinc porphyrin units (DP_m, *m* [number of zinc porphyrin units] = 6, 12, and 24) trap bipyridine compounds carrying multiple fullerene units (Py_2F_n, *n* [number of C_{60} units] = 1−3), affording coordination complexes $DP_m \supset Py_2F_n$ having a photoactive layer consisting of spatially segregated donor and acceptor arrays on their surface. Complexes $DP_m \supset Py_2F_n$ are stable enough (*K* [average binding affinity] = 1.1×10^6−4.4×10^6 M^{-1} in $CHCl_3$ at 25 °C) to be isolated by gel permeation chromatography. UHV−STM microscopy enables clear visualization of a petal-like structure of $DP_{12} \supset Py_2F_3$. Photoexcitation of the zinc porphyrin units in $DP_m \supset Py_2F_n$ results in a zinc porphyrin-to-fullerene electron transfer to generate a charge separation. The charge-separation rate constant (k_{CS}) in CH_2Cl_2 at 20 °C increases from 0.26×10^{10} to 2.3×10^{10} s^{-1} upon increment of *m* and *n*, whereas the charge-recombination rate constant (k_{CR}) remains almost unchanged at 4.5×10^6−6.7×10^6 s^{-1}. Consequently, $DP_{24} \supset Py_2F_3$ furnishes the largest ratio of k_{CS}/k_{CR} (3400) among the family.

Introduction

In biological photosynthesis, photoinduced electron transfer (PET) is one of the most essential events for conversion of solar energy into chemical energy. Molecular design of artificial photosynthetic systems involving restricted spatial arrangements of covalently[1] and noncovalently[2] linked electron donor (D) and acceptor (A) units has long been a central interest and now attracts even greater attention for the development of optoelectronic devices such as solar cells.[3] For the fabrication of those materials, charge-transfer complexations between D and A units, leading to rapid quenching of charge-carrier transports, must be avoided, while D and A units are required to assemble individually to form their segregated arrays.[4] Having this context in mind, we were motivated to achieve at the molecular level such segregated arrays of multiple D and A units. Although a variety of D/A systems having multiple D or A units have been reported,[5] those containing large numbers of both D and A units are unprecedented. In the present paper, we report novel photofunctional dendrimers consisting of spatially segregated arrays of multiple D and A units on their surface.

Our molecular design strategy (Scheme 1) made use of petal-like dendritic structures as scaffolds[6] to realize a wheel-like or spherical arrangement of multiple zinc porphyrin (P) units (DP_m; m = 6, 12, and 24),[7] which are capable of ligating multiple molecules of bipyridine compounds having 1−3 fullerene (F) units (Py_2F_n; n = 1−3). Since the zinc porphyrin moieties in DP_m are located in the outermost dendritic layer, and the

† ERATO-SORST Nanospace Project, JST.
‡ The University of Tokyo.
§ Yonsei University; responsible for time-resolved spectroscopies.
# Osaka University; responsible for scanning tunneling microscopy.

(1) For books and reviews: (a) Kavarnos, G. J. *Fundamentals of Photoinduced Electron Transfer*; VCH: New York, 1993. (b) Wasielewski, M. R. *Chem. Rev.* **1992**, *92*, 435−461. (c) Gust, D.; Moore, T. A.; Moore, A. L. *Acc. Chem. Res.* **2001**, *34*, 40−48. (d) Guldi, D. M. *Chem. Soc. Rev.* **2002**, *31*, 22−36. (e) Imahori, H. *Org. Biomol. Chem.* **2004**, *2*, 1425−1433.
(2) For reviews: (a) El-Khously, M. E.; Ito, O.; Smith, P. M.; D'Souza, F. *J. Photochem. Photobiol., C* **2004**, *5*, 79−104. (b) D'Souza, F.; Ito, O. *Coord. Chem. Rev.* **2005**, *249*, 1410−1422.
(3) (a) Nunzi, J.-M. *C. R. Phys.* **2002**, *3*, 523−542. (b) Gregg, B. A. *J. Phys. Chem. B* **2003**, *107*, 4688−4698. (c) Grätzel, M. *J. Photochem. Photobiol., C* **2005**, *4*, 145−153.
(4) (a) Yu, G.; Gao, J.; Hummelen, J. C.; Wudl, F.; Heeger, A. J. *Science* **1995**, *270*, 1789−1791. (b) Halls, J. J. M.; Walsh, C. A.; Greenham, N. C.; Marseglia, E. A.; Friend, R. H.; Moratti, S. C.; Holmes, A. B. *Nature* **1995**, *376*, 498−500. (c) Peumans, P.; Yakimov, A.; Forrest, S. R. *J. Appl. Phys.* **2003**, *93*, 3693−3723.
(5) (a) Sadamoto, R.; Tomioka, N.; Aida, T. *J. Am. Chem. Soc.* **1996**, *118*, 3978−3979. (b) Kuciauskas, D.; Liddell, P. A.; Lin, S.; Johnson, T. E.; Weghorn, S. J.; Lindsey, J. S.; Moore, A. L.; Moore, T. A.; Gust, D. *J. Am. Chem. Soc.* **1999**, *121*, 8604−8614. (c) Choi, M.-S.; Aida, T.; Luo, H.; Araki, Y.; Ito, O.; *Angew. Chem., Int. Ed.* **2003**, *42*, 4060−4063. (d) Imahori, H.; Sekiguchi, Y.; Kashiwagi, Y.; Sato, T.; Araki, Y.; Ito, O.; Yamada, H.; Fukuzumi, S. *Eur. Chem. J.* **2004**, *10*, 3184−3196. (e) Jiang, D.-L.; Choi, C.-K.; Honda, K.; Li, W.-S.; Yuzawa, T.; Aida, T. *J. Am. Chem. Soc. Chem.* **2004**, *126*, 12084−12089.

Scheme 1. Molecular Structures of Zinc Complexes of Multiporphyrin Dendrimers DP_m (m = 6, 12, and 24), Fullerene-Appended Bipyridine Ligands Py_2F_n (n = 1−3), and Reference Compounds P_1 and Py_2, and Schematic Representation of the Complexation of DP_{24} with Py_2F_3

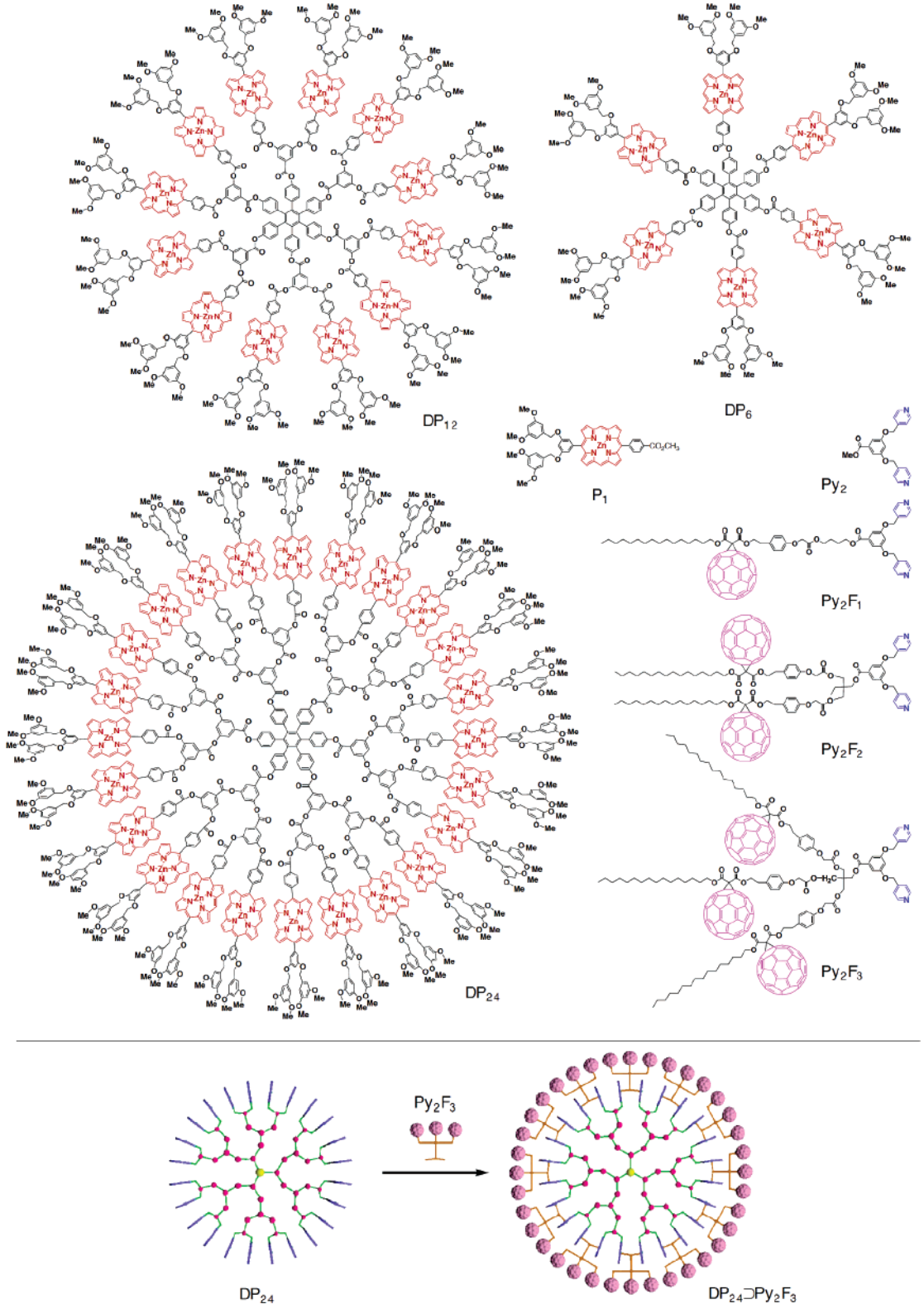

bipyridine and fullerene units in Py_2F_n are apart by roughly 2−3 nm from one another, the coordination of Py_2F_n to DP_m is expected to form a photoactive layer consisting of spatially segregated arrays of multiple donor (zinc porphyrin) and acceptor (fullerene) units on the dendrimer surface. Molecular design of DP_m was inspired by the unique structures of light-harvesting antenna complexes such as LH1 and LH2 in purple bacteria,[8] where multiple bacteriochlorophyll units are spatially arranged like a wheel and ensure efficient harvesting of dilute photons. The excitation energy captured by one of the bacteriochlorophyll unit migrates, without dissipation, to neighboring chlorophyll units in the same and connecting wheel-like chromophore arrays and is subsequently funneled to the photosynthetic reaction center, thereby triggering an electron

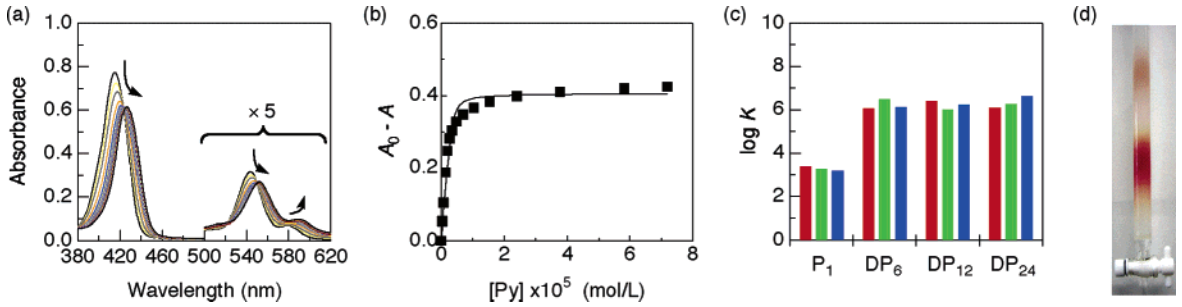

Figure 1. (a) Absorption spectral change of DP_{24} (1.5×10^{-7} M) upon titration with Py_2F_3 ([Py_2F_3]/[DP_{24}] = 0, 1.1, 2.3, 4.6, 6.8, 9.1, 11, 16, 23, 34, 52, 80, 126, 194, and 240) in $CHCl_3$ at 25 °C. (b) Change in absorbance ($A_0 - A$) of DP_{24}, monitored at 415.0 nm, as a function of [Py] (=2 × [Py_2F_3]), and its fitting profile. (c) Binding affinities (log K) of the pyridine units in Py_2F_1 (red), Py_2F_2 (green), and Py_2F_3 (blue) toward the zinc porphyrin units in P_1, DP_6, DP_{12}, and DP_{24} in $CHCl_3$ at 25 °C. (d) A snapshot of gel permeation chromatography (GPC) of a mixture of DP_{24} and Py_2F_3 ([Py_2F_3]/[DP_{24}] = 25) with $CHCl_3$ as an eluent.

transfer. We and other groups have reported that some dendritic multiporphyrin arrays including DP_m, upon photoexcitation, display highly efficient energy migration characteristics analogous to those of the biological light-harvesting systems.[6a,9] Hence, we decided to make use of zinc complexes of multiporphyrin dendrimers DP_m with a certain structural rigidity for an attempt to construct a concentric double layer of spatially segregated arrays composed of multiple D and A units (Scheme 1). As an electron acceptor for DP_m, we chose a fullerene such as C_{60} because of its small reorganization energy and excellent electron-accepting properties.[10] Thus, we synthesized Py_2F_n having 1−3 fullerene units (n = 1−3), where the bipyridine (Py_2) unit was expected to coordinate strongly in a bidentate fashion to two neighboring zinc porphyrin units in DP_m, thereby allowing the formation of a fullerene array outside of the zinc porphyrin array on the dendrimer surface ($DP_m \supset Py_2F_n$). Here, one can change the packing densities of these D and A units in the photoactive layer by varying the m and n values in the DP_m and Py_2F_n components, respectively, and might therefore be able to modulate the photoinduced charge-separation event.

Results and Discussion

Zinc complexes of multiporphyrin dendrimers DP_m (m = 6, 12, and 24) were synthesized according to a method analogous to that reported previously for chiroptical sensing of chiral bipyridine compounds.[7] On the other hand, fullerene-appended bipyridine ligands Py_2F_n (n = 1−3) were synthesized by coupling of a fullerene-containing carboxylic acid precursor with bipyridine-terminated alcohols bearing 1−3 hydroxyl groups.[11] In $CHCl_3$, DP_6 showed an absorption spectral profile typical of 5,15-diarylporphyrin zinc complexes, having a Soret absorption band centered at 414 nm and Q-bands at 542 and 578 nm. Compared with DP_6, DP_{24} showed a broad Soret absorption band centered at 415 nm, while DP_{12} showed a blue-shifted shoulder at 398 nm along with a major Soret band at 411 nm. The latter observation suggests that DP_{12} may adopt a planar geometry with a H-aggregate-type arrangement of the zinc porphyrin units along its periphery.[7] On the other hand, Py_2F_1−Py_2F_3 all displayed an electronic absorption band centered at 326 nm.[11] Upon excitation at 326 nm, all Py_2F_n fluoresced at 694 nm from their fullerene units.[10,11]

As expected, DP_m (m = 6, 12, and 24) bound Py_2F_n (n = 1−3) strongly to form stable $DP_m \supset Py_2F_n$. For example, upon titration with Py_2F_3 in $CHCl_3$ at 25 °C, DP_{24} (1.5×10^{-7} M) displayed a large spectral change in the Soret and Q-bands (Figure 1a), characteristic of the axial coordination of zinc porphyrins, with a clear saturation profile at a molar ratio [Py_2F_3]/[DP_{24}] exceeding 12 (Figure 1b). This spectral change profile did not give distinct isosbestic points possibly due to a large effect of the multivalency of the complexation between DP_{24} and Py_2F_3. However, the average binding affinity (K), as estimated by simply assuming a one-to-one coordination between the individual zinc porphyrin and pyridine units, was 1.2×10^6 M^{-1}.[11] This value is more than 2 orders of magnitude greater than association constants reported for monodentate coordination between zinc porphyrins and pyridine derivatives.[12] Other combinations of DP_m and Py_2F_n for the titration all showed analogous spectral change profiles with a marked saturation tendency at a mole ratio [Py_2F_n]/[DP_m] close to m/2.[11] Figure 1c shows average binding affinities K between the zinc porphyrin and pyridine units, which are almost comparable to one another in a range 1.1×10^6−4.4×10^6 M^{-1} irrespective of the m and n values in DP_m and Py_2F_n, respectively. We also found that resulting complexes $DP_m \supset Py_2F_n$ are all stable under conditions for gel permeation chromatography (GPC). For example, a $CHCl_3$ solution (0.5 mL) of a mixture of DP_{24} and Py_2F_3 ([DP_{24}] = 1.6×10^{-5} M, [Py_2F_3]/[DP_{24}] = 25) was loaded onto a Bio-beads S-X1 GPC column and then eluted with $CHCl_3$. As shown in Figure 1d, the chromatographic profile

(6) For dendritic multiporphyrin arrays: (a) Yeow, E. K. L.; Ghiggino, K. P.; Reek, J. N. H.; Crossley, M. J.; Bosman, A. W.; Schenning, A. P. H. J.; Meijer, E. W. *J. Phys. Chem. B* **2000**, *104*, 2596−2606. (b) Choi, M.-S.; Aida, T.; Yamazaki, T.; Yamazaki, I. *Angew. Chem., Int. Ed.* **2001**, *40*, 3194−3198. (c) Choi, M.-S.; Aida, T.; Yamazaki, T.; Yamazaki, I. *Chem. Eur. J.* **2002**, *8*, 2667−2678. (d) Benites, M. R.; et al. *J. Mater. Chem.* **2002**, *12*, 65−80. (e) Choi, M.-S.; Yamazaki, T.; Yamazaki, I.; Aida, T. *Angew. Chem., Int. Ed.* **2004**, *43*, 150−158. (f) Imahori, H. *J. Phys. Chem. B* **2004**, *108*, 6130−6143. (g) Solladié, N., Sooambar, C., Herschbach, H., Strub, J.-M., Leize, E., Van Dorsselaer, A., Talarico, A. M., Ventura, B., Flamigni, L. *New J. Chem.* **2005**, *29*, 1504−1507.

(7) Li, W.-S.; Jiang, D.-L.; Suna, Y.; Aida, T. *J. Am. Chem. Soc.* **2005**, *127*, 7700−7702.

(8) (a) Mcdermott, G.; Prince, S. M.; Freer, A. A.; Hawthornthwaite-Lawless, A. M.; Papiz, M. Z.; Cogdell, R. J.; Isaacs, N. W. *Nature* **1995**, *374*, 517−521. (b) Karrasch, S.; Bullough, P. A.; Ghosh, R. *EMBO J.* **1995**, *14*, 631−638. (c) Pullerits, T.; Sundström, V. *Acc. Chem. Res.* **1996**, *29*, 381−389.

(9) (a) Cho, S.; Li, W.-S.; Yoon, M.-C.; Ahn, T. K.; Jiang, D.-L.; Kim, J.; Aida, T.; Kim, D. *Chem. Eur. J.*, in press. (b) Fujitsuka, M.; Hara, M.; Tojo, S.; Okada, A.; Troiani, V.; Solladié, N.; Majima, T. *J. Phys. Chem. B* **2005**, *109*, 33−35.

(10) (a) Guldi, D. M.; Prato, M. *Acc. Chem. Res.* **2000**, *33*, 695−703. (b) Guldi, D. M. *Chem. Commun.* **2000**, 321−327. (c) Thomas, K. G.; George, M. V. *Helv. Chim. Acta* **2005**, *88*, 1291−1308.

(11) See Supporting Information.

(12) Sanders, J. K. M.; Bampos, N.; Clyde-Watson, Z.; Darling, S. L.; Hawley, J. C.; Kim, H.-J.; Mak, C. C.; Webb, S. J. In *Axial Coordination Chemistry of Metalloporphyrins*; Kadish, K. M., Smith, K. M., Guilard, R., Eds.; The Porphyrin Handbook; Academic Press: San Diego, 2000; Vol. 3, p 30.

Table 1. Average Numbers of Py_2F_n Bound to Single DP_m Molecule in $DP_m \supset Py_2F_n$, upon Mixing DP_m with Py_2F_n ($[Py_2F_n]/[DP_m] = m$) in $CHCl_3$ at 25 °C, Followed by GPC Separation with $CHCl_3$ as an Eluent (Figure 1d)[11]

	Py_2F_1	Py_2F_2	Py_2F_3
DP_6	2.9	2.6	2.6
DP_{12}	5.3	5.5	5.3
DP_{24}	9.0	9.6	9.5

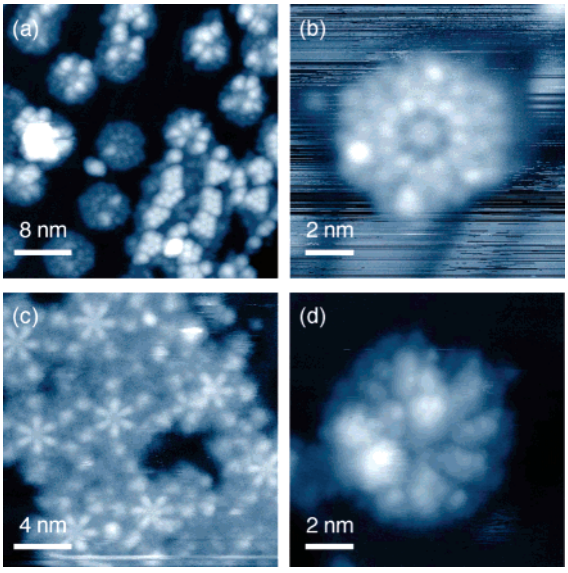

Figure 2. UHV−STM micrographs of (a, b) DP_{12} in the presence of 6 equiv of Py_2F_3, (c) DP_6 in the presence of 3 equiv of Py_2F_1, and (d) DP_{24} in the presence of 12 equiv of Py_2F_1, on a Au(111) surface at a liquid nitrogen temperature. Conditions: (a) $I = 1$ pA, $Vs = +3$ V; (b) $I = 1$ pA, $Vs = +2$ V; (c) $I = 2$ pA, $Vs = +4.5$ V; (d) I = 1 pA, $Vs = +2$ V.

displayed two colored fractions. By means of absorption spectroscopy, the first fraction was found to contain both DP_{24} and Py_2F_3 at a molar ratio $[Py_2F_3]/[DP_{24}]$ of 9.5 (Table 1), whereas the second fraction included Py_2F_3 alone.[11] The observed ratio of $[Py_2F_3]/[DP_{24}]$ is fairly close to an expected ratio of 12 for the bidentate ligation of Py_2F_3 to the zinc porphyrin units in DP_{24}. As summarized in Table 1, we likewise isolated by GPC $DP_m \supset Py_2F_n$ formed from the other combinations of DP_m and Py_2F_n and confirmed from their compositions that almost all the zinc porphyrin units in DP_m participate in the bidentate ligation with Py_2F_n. In contrast, P_1, a nondendritic zinc porphyrin reference (Scheme 1), incapable of bidentate ligation with Py_2F_n, exhibited much smaller binding affinities ($\sim 2.0 \times 10^3$ M^{-1}) toward $Py_2F_1-Py_2F_3$ (Figure 1c).

We succeeded in visualizing some of the coordination complexes between DP_m and Py_2F_n by scanning tunneling microscopy under ultrahigh vacuum conditions (UHV−STM). For example, when a $CHCl_3$ solution of a mixture of DP_{12} and Py_2F_3 ($[DP_{12}] = 2.0 \times 10^{-6}$, $[Py_2F_3]/[DP_{12}] = 8.2$) was deposited on a Au(111) surface by pulse injection,[13] UHV−STM at a liquid nitrogen temperature displayed petal-like patterns with a uniform diameter of 7 nm, assignable to DP_{12} adopting a planer conformation on the substrate surface (Figures 2a and 2b). UHV−STM also exhibited many bright spots at the periphery of DP_{12} molecules, which are most likely fullerene clusters of Py_2F_3. While $DP_6 \supset Py_2F_1$ showed a petal-like pattern

(13) (a) Tanaka, H.; Kawai, T. *J. Vac. Sci. Technol. B* **1997**, *15*, 602−604. (b) Tanaka, H.; Kawai, T. *Surf. Sci.* **2003**, *539*, L531−L536.

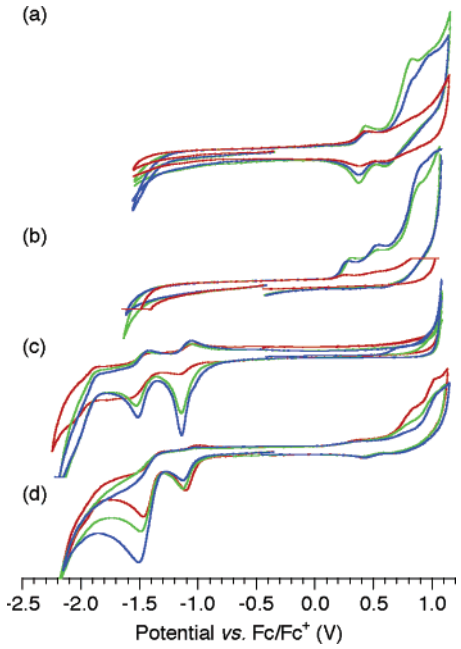

Figure 3. Cyclic voltammograms of (a) DP_6 (green), DP_{12} (blue), and DP_{24} (red) alone, (b) those in the presence of Py_2 ([pyridine]/[zinc porphyrin] = 1), (c) Py_2F_1 (red), Py_2F_2 (green), and Py_2F_3 (blue) alone, and (d) those in the presence of DP_{12} ([pyridine]/[zinc porphyrin] = 1). Conditions: 0.1 M $Bu_4N^+PF_6^-$ as a supporting electrolyte, scan rate: 100 mV/s, Pt electrodes, in CH_2Cl_2 at 25 °C.

(Figure 2c), the complex likely lost most of the ligating Py_2F_1 molecules during the process for pulse injection. On the other hand, as shown in Figure 2d, $DP_{24} \supset Py_2F_1$ in UHV−STM developed a rather obscure molecular image, possibly due to a difficulty of large DP_{24} in flattening on the substrate surface.

Electrochemical properties of DP_m, Py_2F_n, and reference complexes for $DP_m \supset Py_2F_n$ were investigated by means of cyclic voltammetry (CV). In CH_2Cl_2 at 25 °C, DP_6, DP_{12}, and DP_{24} displayed nearly identical redox properties to one another with the first oxidation potential ($E_{Ox}^{0/\cdot+}$) at around 0.40 V versus Fc/Fc^+ (Figure 3a). For the evaluation of the redox potentials of the pyridine-ligating zinc porphyrin units in $DP_m \supset Py_2F_n$, we utilized, in place of Py_2F_n, reference bipyridine compound Py_2 without fullerene units (Scheme 1). Upon addition of 3 equiv of Py_2 to a CH_2Cl_2 solution of DP_6, the oxidation peak, as expected, showed a cathodic shift down to $E_{Ox}^{0/\cdot+}$ of 0.28 V due to an electron donation from ligating Py_2 to the zinc porphyrin units (Figure 3b). A similar electronic effect of Py_2 was observed for the oxidation potentials of DP_{12} and DP_{24}, although the extent of such a cathodic shift was a little more explicit as the steric congestion of the dendrimer became larger: $E_{Ox}^{0/\cdot+} = 0.26$ (DP_{12}) and 0.23 V (DP_{24}). On the other hand, Py_2F_n showed the first reduction potential ($E_{Red}^{0/\cdot-}$) at −1.08 ($n = 1$), −1.10 ($n = 2$), and −1.10 ($n = 3$) versus Fc/Fc^+ in CH_2Cl_2 (Figure 3c), which remained virtually intact upon complexation with DP_m such as DP_{12} (Figure 3d).

Photoinduced electron transfer in $DP_m \supset Py_2F_n$ was confirmed by means of steady-state emission spectroscopy and nanosecond flash photolysis measurements. For example, excitation of a $CHCl_3$ solution of DP_{24} (1.5×10^{-7} M) at 550 nm resulted in a fluorescence emission from the zinc porphyrin units at 591 and 635 nm (Figure 4a). Upon titration with Py_2F_3, the fluorescence stepwise decreased in intensity and was quenched almost completely in the final stage. Stern−Volmer constants

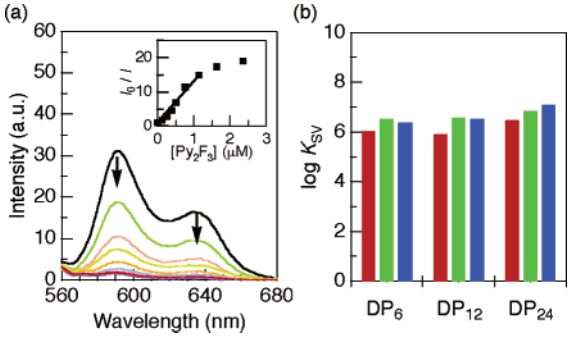

Figure 4. (a) Fluorescence spectral change and Stern−Volmer plot (inset) of DP_{24} (1.5×10^{-7} M) upon excitation at 550 nm in the presence of Py_2F_3 ([Py_2F_3]/[DP_{24}] = 0, 0.85, 1.7, 2.6, 3.4, 5.1, 7.7, 11, and 16 in $CHCl_3$ at 25 °C under Ar. (b) Stern−Volmer constants of DP_6, DP_{12}, and DP_{24} in the presence of Py_2F_1 (red), Py_2F_2 (green), and Py_2F_3 (blue).

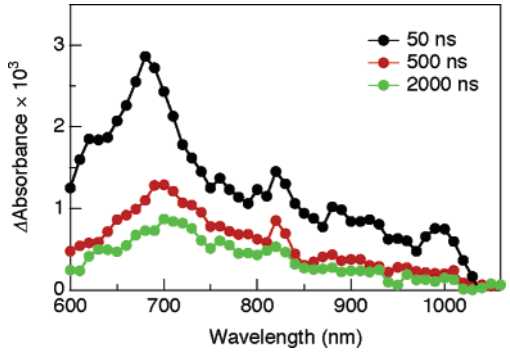

Figure 5. Nanosecond transient absorption spectra at 20 °C of a CH_2Cl_2 solution of DP_6 (1.7×10^{-5} M) containing 3 equiv of Py_2F_3 upon photoexcitation at 532 nm.

(K_{SV}, Figure 4b),[11] evaluated for the combination of DP_m (m = 6, 12, and 24) and Py_2F_n (n = 1−3), were roughly comparable to their average binding affinities K (Figure 1c), indicating that the fluorescence quenching of DP_m is caused by the coordination of electron-accepting Py_2F_n. By means of transient absorption spectroscopy, we confirmed the occurrence of an electron transfer from the photoexcited zinc porphyrin units in DP_m to the fullerene units in ligating Py_2F_n. Excitation of a CH_2Cl_2 solution of DP_6 (1.7×10^{-5} M) at 532 nm in the presence of 3 equiv of Py_2F_3 resulted in a transient absorption spectrum (Figure 5) with bands at around 680 and 1000 nm assignable to the cation and anion radicals of the zinc porphyrin and fullerene units, respectively. Broad absorption bands, observed at 750−900 nm, are due to the excited triplet states of these two units. Since the fluorescence spectral profiles of $DP_m \supset Py_2F_n$ such as $DP_6 \supset Py_2F_3$ under the conditions employed here did not show any sign of energy transfer from the photoexcited zinc porphyrin units in DP_m to the fullerene units of Py_2F_n,[11,14] we conclude that the quenching of the zinc porphyrin fluorescence observed for $DP_m \supset Py_2F_n$ (Figure 4) is mostly due to the intracomplex photoinduced electron transfer between them.

Time-resolved emission spectroscopy was employed for investigating the charge-separation event in $DP_m \supset Py_2F_n$.[11] Upon excitation at 420 nm in CH_2Cl_2 at 20 °C, the fluorescence of DP_6 (1.0×10^{-6} M) in the presence of 3 equiv of fullerene-free bipyridine displayed a monoexponential decay profile at 590 nm with a lifetime (τ_f) of 1.6 ns. On the other hand, when

(14) Kuciauskas, D.; Lin, S.; Seely, G. R.; Moore, A. L.; Moore, T. A.; Gust, D.; Drovetskaya, T.; Reed, C. A.; Boyd, P. D. W. *J. Phys. Chem.* **1996**, *100*, 15926−15932.

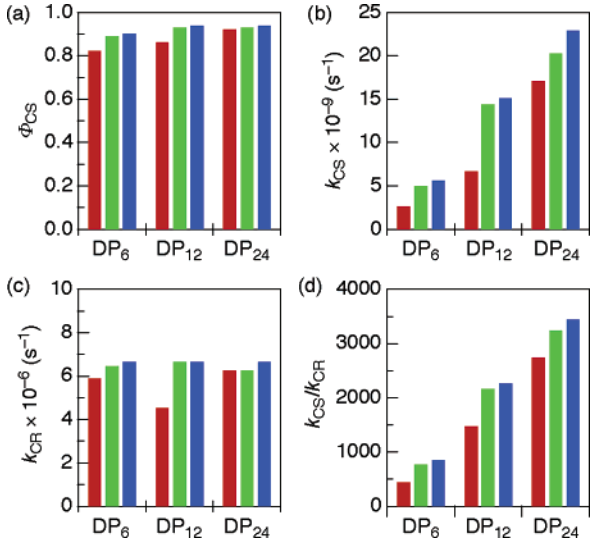

Figure 6. (a) Charge-separation quantum yields (Φ_{CS}), (b) charge-separation rate constants (k_{CS}), (c) charge-recombination rate constants (k_{CR}), and (d) k_{CS}/k_{CR} of DP_6, DP_{12}, and DP_{24} in the presence of Py_2F_1 (red), Py_2F_2 (green), and Py_2F_3 (blue) in CH_2Cl_2 at 20 °C.

fullerene-appended Py_2F_1 was used in place of Py_2, a fast-decay fluorescing component with τ_f of 320 ps appeared in addition to the slow-decay component (τ_f = 1.1 ns). This fast-decay component obviously originates from the charge-separation process caused by the photoinduced electron transfer from DP_6 to Py_2F_1. In the presence of Py_2F_2 or Py_2F_3 instead of Py_2F_1, the lifetime of the fast-decay component of DP_6 became much shorter; τ_f = 170 (Py_2F_2) and 150 ps (Py_2F_3). In contrast with $DP_6 \supset Py_2$, $DP_{12} \supset Py_2$ and $DP_{24} \supset Py_2$ exhibited a biexponential fluorescence decay at 590 nm possibly due to a dense packing of the zinc porphyrin units (vide ante) on the dendrimer surface.[11] Use of Py_2F_n in place of Py_2 to allow complexation with DP_{12} or DP_{24} resulted in an additional decay component with a much shorter τ_f value, owing to the electron transfer from DP_m to Py_2F_n.[11] On the basis of the fluorescence decay profiles, the charge-separation rate constants (k_{CS}) and quantum yields (Φ_{CS}) were evaluated according to the following equations by comparison of the shortest τ_f components of $DP_m \supset Py_2F_n$ with average τ_f values of $DP_m \supset Py_2$:

$$k_{CS} = \left(\frac{1}{\tau_f}\right)_{DP_m \supset Py_2F_n} - \left(\frac{1}{\tau_f}\right)_{DP_m \supset Py_2}$$

$$\Phi_{CS} = \left[\left(\frac{1}{\tau_f}\right)_{DP_m \supset Py_2F_n} - \left(\frac{1}{\tau_f}\right)_{DP_m \supset Py_2}\right] \Big/ \left(\frac{1}{\tau_f}\right)_{DP_m \supset Py_2F_n}$$

The Φ_{CS} values thus evaluated are all high, ranging from 0.82 to 0.94 (Figure 6a). Thus, the photoinduced electron transfer in $DP_m \supset Py_2F_n$ occurred very efficiently, irrespective of the magnitudes of m and n. Of further interest, the k_{CS} value increases following the order of $Py_2F_1 < Py_2F_2 < Py_2F_3$ and enhances, to a much greater extent, from DP_6 to DP_{12} and then to DP_{24} (Figure 6b). For example, the k_{CS} value of 2.3×10^{10} s^{-1}, as evaluated for $DP_{24} \supset Py_2F_3$, is an order of magnitude greater than that of $DP_6 \supset Py_2F_1$ (0.26×10^{10} s^{-1}) and obviously the largest among those of the $DP_m \supset Py_2F_n$ family. These trends indicate an interesting possibility that dense packing of both the zinc porphyrin and fullerene units on the dendrimer surface

plays an essential role in facilitating the charge-separation process. As expected, nondendritic zinc porphyrin reference P_1 in the presence of Py_2F_n showed much smaller k_{CS} values such as 0.031×10^{10} ($n = 1$), 0.12×10^{10} ($n = 2$), and 0.13×10^{10} s^{-1} ($n = 3$).

We also investigated the charge-recombination events in $DP_m \supset Py_2F_n$, using the decay profiles in CH_2Cl_2 of the transient absorption band at 1000 nm due to $C_{60}^{\bullet -}$ (Figure 5).[11] In every case, the decay profile was satisfactorily fitted with two-exponential components, where the faster decay is attributed to the charge-recombination process, while the slower decay originates from the excited triplet species. The charge-recombination rate constants (k_{CR}, Figure 6c) thus obtained are all within a narrow range from 4.5×10^6 to 6.7×10^6 s^{-1}, and the lifetimes of the charge-separation state (τ_{RIP}; 150−220 ns) are comparable to one another.[11] These trends are quite reasonable since the donor−acceptor distance in $DP_m \supset Py_2F_n$ should not be much dependent on the degrees of steric congestion of the two ligating components but is primarily determined by the length of the spacer unit between the bipyridine and fullerene units in Py_2F_n. The successful determination of the k_{CS} values for $DP_m \supset Py_2F_n$ allowed us to compare the ratios of k_{CS}/k_{CR}, which have often been used as a measure for the excellence of photoinduced electron-transfer systems.[15] Of interest, the values of k_{CS}/k_{CR} (Figure 6d) are all large in a range from 450 ($DP_6 \supset Py_2F_1$) to 3400 ($DP_{24} \supset Py_2F_3$). In particular, the k_{CS}/k_{CR} ratio for $DP_{24} \supset Py_2F_3$ is more than an order of magnitude greater than those reported for precedent porphyrin−fullerene supramolecular dyads and triads.[15] It is obvious that a larger number of the fullerene units in $DP_{24} \supset Py_2F_3$ could enhance the probability of the electron transfer from the zinc porphyrin units. However, in addition to this, one can also presume that an efficient energy migration along the densely packed zinc porphyrin array[9] may enhance the opportunity for this electron transfer. When the degrees of fluorescence quenching ($1 - I/I_0$) [I and I_0; fluorescence intensities with and without the quencher, respectively], observed for DP_6, DP_{12}, and DP_{24} upon titration with Py_2F_3, are plotted against the ratio of the numbers of the fullerene and zinc porphyrin units ([fullerene]/[zinc porphyrin]),[11] it is clear that the quenching of the excited singlet state of the zinc porphyrin units by Py_2F_3 is more efficient as m in DP_m is larger from 6 to 12 and then to 24 (Figure 7). For example, the degree of fluorescence quenching of 0.6 can be attained for DP_{24} only at [fullerene]/[zinc porphyrin] = 0.19, whereas it requires a much larger ratio of [fullerene]/[zinc porphyrin] such as 0.64 for DP_6. Since the average binding affinities of Py_2F_3 toward DP_6 and DP_{24} are not much different from one another (Figure 1c), it is obvious that the energy migration along the zinc porphyrin array in DP_{24}[9] greatly facilitates the electron transfer to the fullerene units.

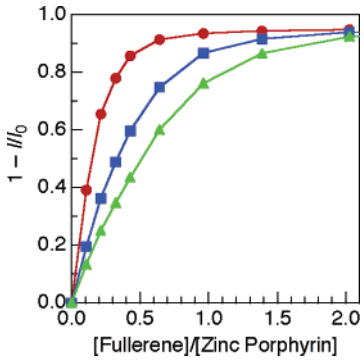

Figure 7. Plots of degrees of fluorescence quenching ($1 - I/I_0$) versus [fullerene]/[zinc porphyrin] upon titration of DP_6 (green), DP_{12} (blue), and DP_{24} (red) ([zinc porphyrin] = 3.6×10^{-6} M) with Py_2F_3 in $CHCl_3$ at 25 °C. Concentrations of fullerene and zinc porphyrin units are given by $3 \times$ [Py_2F_3] and $m \times$ [DP_m], respectively.

Conclusions

By means of a multivalent surface ligation of dendritic macromolecules,[16] we constructed, using DP_m ($m = 6$, 12, and 24) and Py_2F_n ($n = 1-3$), a photoactive layer, consisting of electron-donating zinc porphyrin and electron-accepting fullerene arrays on the dendrimer surface. Upon increment of the numbers of these donor and acceptor units, the electron transfer reaction was remarkably facilitated, while the recombination of the resulting charge-separated state remained virtually intact. Consequently, among the $DP_m \supset Py_2F_n$ family, $DP_{24} \supset Py_2F_3$ accommodating 24 zinc porphyrin units and roughly 30 fullerene units on the dendrimer surface (Table 1) achieved the largest ratio of the charge-separation to charge-recombination rate constants (3400), which is even 1 order of magnitude greater than those of precedent examples. Application of this molecular design strategy to the development of optoelectronic materials is one of the subjects worthy of further investigations.

Acknowledgment. We are grateful to Dr. Yohei Yamamoto for STM measurements. D.K. acknowledges the financial support through the Star Faculty Program of the Ministry of Education and Human Resources.

Supporting Information Available: Details for synthesis, characterization, and spectral data (PDF). This material is available free of charge via the Internet at http://pubs.acs.org. See any current masthead page for ordering information and Web access instructions.

JA063081T

(15) (a) D'Souza, F.; Gadde, S.; Zandler, M. E.; Arkady, K.; El-Khouly, M. E.; Fujitsuka, M.; Ito, O. *J. Phys. Chem. A* **2002**, *106*, 12393−12404. (b) D'Souza, F.; Deviprasad, G. R.; Zandler, M. E.; El-Khouly, M. E.; Fujitsuka, M.; Ito, O. *J. Phys. Chem. A* **2003**, *107*, 4801−4807. (c) D'Souza, F.; Smith, P. M.; Gadde, S.; McCarty, A. L.; Kullman, M. J.; Zandler, M. E.; Itou, M.; Araki, Y.; Ito, O. *J. Phys. Chem. B* **2004**, *108*, 11333−11343. (d) D'Souza, F.; El-Khously, M. E.; Gadde, S.; McCarty, A. L.; Karr, P. A.; Zandler, M. E.; Araki, Y.; Ito, O. *J. Phys. Chem. B* **2005**, *109*, 10107−10114.

(16) (a) Fréchet, J. M. J. *Proc. Acad. Sci., U.S.A.* **2002**, *99*, 4782−4787. (b) Broeren, M. A. C.; van Dongen, J. L. J.; Pitterlkow, M.; Christensen, J. B.; van Genderen, M. H. P.; Meijer, E. W. *Angew. Chem., Int. Ed.* **2004**, *43*, 3557−3562. (c) van Baal, I.; Malda, H.; Synowsky, S. A.; van Dongen, J. L. J.; Hackeng, T. M.; Merkx, M.; Meijer, E. W. *Angew. Chem., Int. Ed.* **2005**, *44*, 5052−5057. (d) Smith, D. K. *Chem. Commun.* **2006**, 34−44.